Aviation-to-Grid Flexibility through Electric Aircraft Charging

Zekun Guo, *Student Member, IEEE*, Jinning Zhang, Rui Zhang, and Xin Zhang, *Senior Member, IEEE*

Abstract—This paper proposes a new concept of Aviation-to-Grid (A2G) that utilises electric aircraft (EA) charging to provide flexibility to the power grid. Smart EA charging system with battery swap method is developed using Photovoltaics (PV), gas turbine, and grid electricity. Hourly energy dispatch strategy is produced based on the mixed integer linear programming method to meet electrified aviation charging demand and provide A2G frequency response to the power grid. Case studies are conducted in 8 major UK airports considering seasonal flight schedules and power system operation scenarios. Results show that the EA charging system can provide effective primary and secondary frequency response to improve the frequency nadir by 0.2 - 0.3 Hz under grid disturbance. The total A2G frequency response capacity across the 8 UK airports can reach 900 - 1,200 MW overnight and 300 - 900 MW daytime in summer, and 1,100 - 1,300 MW overnight and 200 - 700 MW daytime in winter. The annual A2G frequency response revenue is estimated to be £46.58 million, which can cover 19.8% to 30% of EA charging costs.

Index Terms— Air transport electrification, electric aircraft charging, power grid, frequency response, mixed integer linear programming

I. INTRODUCTION

Electric aircraft (EA) has been identified as one of the promising approaches to reduce CO2 emissions and NOx pollution for aviation industry. Significant number of research has focused on the EA on-board power system technologies [1]. However, the EA charging will have significantly impact on ground power systems, in particular the extra charging demand and infrastructure. The study in [2] indicates that the global electricity consumption will increase by 112-344 TWh

Zekun Guo and Xin Zhang are with the Brunel Interdisciplinary Power Systems Research Centre, Department of Electronic and Electrical Engineering, Brunel University London, London, UB8 3PH, UK (email: zekun.guo@brunel.ac.uk; xin.zhang@brunel.ac.uk).

Jinning Zhang is with the Centre for Propulsion, School of Aerospace, Transport and Manufacturing, Cranfield University, Bedford, MK43 0AL, UK (email: jinning.zhang@cranfield.ac.uk).

Rui Zhang is with the Electricity National Control Centre, National Grid ESO, Wokingham, RG41 5BN, UK (email: rui.zhang@nationalgrideso.com)

(0.6-1.7% of 2015 global electricity consumption) if all the short haul flights with 400-600 nautical-mile (nm) are operated by all-electric aircraft. In the UK, additional 1.2-3.6 GW electricity generation capacity is required even if the daily first morning flight is electrified which requires the EA batteries to be recharged overnight. Electric aircraft such as air taxis with 1-4 passengers over a distance of around 100 km require battery specific energy of 200Wh/kg [2]. The existing fast charger (10-50kW) for electric vehicle is not quick enough for aircraft charging (4-20 hours) due to the high-power consumptions of aircraft propulsion system and constrained flight turnaround time. However, the EA charging has potentials to provide grid flexibility through the large EA batteries and their charging infrastructure.

One key challenge for power system operators is the real time balancing of electricity generation and demand. The imbalance between generation and load will be reflected in frequency deviation of the power system [3]. The inertia stored in the synchronous generators can reduce the frequency deviation. However, with the increasing penetration of renewable power generation which is expected to reach over 60% in the future GB power grid [4], the system inertia will reduce significantly due to the power electronics-interfaced renewable energy that do not provide conventional inertia to the grid. Therefore, the real-time balancing mechanism will require additional frequency response services through the new flexibility-enabled energy sources.

The frequency response services are mainly provided by the conventional generation units [5]. With the increasing penetration level of renewable power generation that is replacing the conventional synchronous machines, the system inertia will reduce significantly caused by less synchronous machines that contain rotational kinetic energy [6]. Therefore new and additional frequency response services are urgently required for frequency stability in a low-inertia power system [7]. Various frequency control methods have been proposed. A novel tuning method is proposed which enables the fuzzy hierarchal control structure to supplement the conventional control and improve the power system stability and robustness [8].

Battery swap is a technology that directly swaps the empty batteries from the arrival vehicles with a fully-charged battery. The empty batteries will be charged off-board in a scheduled period when the power system is not in congestion. As a result, battery swap is recognized as a flexible charging strategy particularly for large capacity batteries. This concept has been
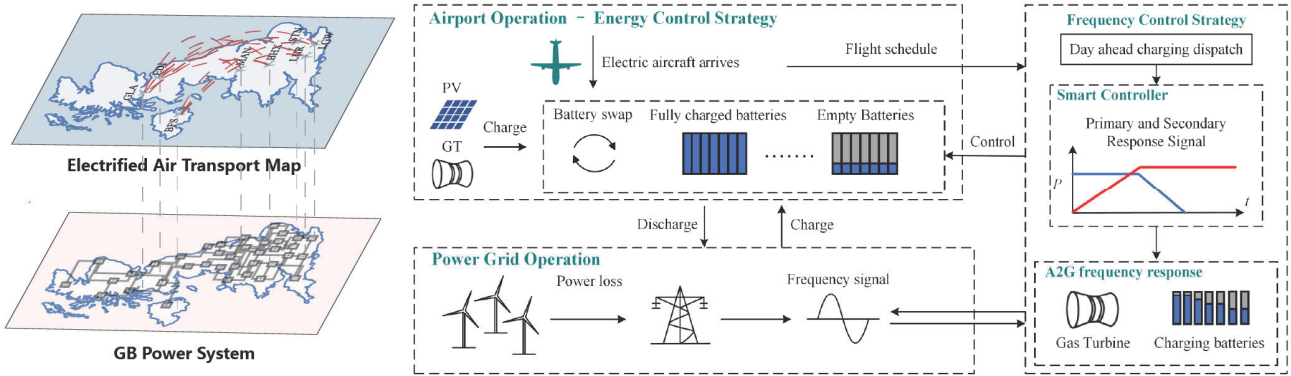
Fig. 1. A new nexus between electrified air transport and electrical power systems - Electric aircraft charging system with grid frequency response

widely researched in electric public transportation. In most of the existing literatures, the battery swap process is formulated by various linear integer or mixed integer program with different optimization algorithms to solve this problem. a population-based evolutionary algorithm is proposed to optimize the allocation of distributed generation and battery swap stations [9]. An electric vehicle transportation network routing problem is presented with battery swapping stations located in the city [10]. Battery swap is adopted to recharge a fleet of electric commuter aircraft aiming to minimize the operation costs and charging infrastructure expenditures [11]. The battery swap process is formulated with a state flow model and to assess the operation cost of the battery swap station [12][13][14]. Based on the literature review, this paper selects the state flow model to formulate the battery swap process and evaluate the potential of the flexibility provided by the EA charging system.

Many existing studies have been carried out to investigate the potential distributed energy resources to provide frequency regulation services. As one major type of distributed energy resources in the future, micro gas turbines could provide firm frequency response services. In [15], the operational flexibility of different types of gas turbines have been reviewed in particular the future technologies that improve the performance in ramp-up rates, start-up rates and compliant load. These improved characteristics will enable the gas turbines to provide highly effective frequency response ability. In recent years there has been growing interests in adopting EVs for grid frequency response service [16][17]. In [16], two frequency control modes of EVs are compared: one is to load-shedding of EV charging in the frequency contingency, the other control mode is to discharge the EV batteries to the grid. The results in [17] indicate that the frequency deviation caused by the wind energy uncertainties will be significantly reduced by the utilisation of EVs for the dynamic frequency control. [18] proposed a hierarchically adaptive frequency control for power system with EV and renewable energy units. In most of literature reviews, the primary frequency response and secondary response are usually separated, and the response service is normally provided by a single type of energy resources. In this paper, a coordinative frequency response service which provides both primary and secondary frequency response is developed for electrified air transport – power

systems nexus.

The originality of this work is to combine the state flow model, gas turbine operation model and frequency response scheme. The basic theory of the battery swap model is "state flow", which means there are time-series matrices to describe the SoC of the batteries in each state (charging, idling, fully charged). At the moment, we focus on the novel application of state flow model into electric aircraft (EA) charging, there are significant differences between EV and EA in terms of quantity, battery capacity, and operation strategy, in particular the EV has a customer-driven operation behaviour while the EA has centrally managed and highly scheduled operation strategy. To fit the whole EA charging system into grid frequency response scheme, we have also introduced additional gas turbine operation parameters to fit in the battery swap state flow model.

To address the challenges in high-power and highly-scheduled EA charging as well as to explore the new flexibility provisions from EA charging, we propose a new concept of 'Aviation-to-Grid (A2G)' flexibility to utilise EA battery charging system to provide frequency response for frequency regulation. The A2G frequency response services will be further enhanced by coordinating with airport gas turbines which are primarily used to provide off-grid and high-power charging to the swappable EA batteries. The main contributions of this paper are:

- An EA charging system is developed to handle highly-scheduled charging patterns that are driven from the electrified air transport. The developed charging system is able to accommodate high-power charging in a short flight turnaround time at airports.
- A novel Aviation-to-Grid (A2G) concept that uses EA charging as a new energy resource to provide flexibility to the power grid. Coordinated energy control solutions of EA batteries and gas turbines will provide combined primary and secondary frequency responses to grid disturbance.

II. ELECTRIFIED AIR TRANSPORT – POWER SYSTEMS NEXUS

A. Aviation-to-Grid concept and motivation

Currently, there is a significant disconnect between power systems and electrified air transport in terms of energy users and suppliers, infrastructure and interoperability to achieve net-zero in both industries. As shown in Fig. 1, the

electrification of aviation will create a new 'nexus' between power systems and electrified air transport through electrification, with potentials to enable a novel technology of 'Aviation-to-Grid flexibility'. There are several key problems to be solved:

• The power systems will require electrified aviation to integrate into ground energy infrastructure and must not overload the future grid.

• Electrified aviation as a new energy user requires the power systems to supply large volumes of low-carbon electricity to meet new loads of electric aircraft.

• Significant charging infrastructures are required. Our feasibility study on Gatwick airport indicates that even if only 10% domestic flights are electrified then £50M will need to be spent on charging infrastructure [19]. Significantly high costs will also be incurred for building additional power generation capacity.

B. Aviation-to-Grid as a new nexus between power systems and electrified air transport

As shown in Fig. 1, this research paper will explore the fundamental integration of Aviation-to-Grid as the new nexus between electrical power and electrified air transport systems, Aviation-to-Grid is defined to include various levels and locations of integration between power system and electrified air transport system, from individual airports as well as national power system operation. Aviation-to-Grid flexibility is proposed as the ability that the electrified air transport can adjust, with an acceptable ramp rate in a defined boundary, to maintain electricity supply and demand in its own system as well as to support the power systems frequency response. Aviation-to-Grid flexibility will be investigated as a key solution for effective costs reduction in terms of energy purchase costs and frequency response services in both power and aviation industries, which will achieve low-carbon energy supply to electrified aviation at affordable costs from power grid. There are around 50 commercial airports with a large number of domestic and international flights in the UK. As the adoption of EA requires intensive investment on electric charging infrastructure, the top 8 busiest UK airports are assumed to be the first batch of airports to be electrified. In addition, due to the battery energy density and range anxiety of EA, only domestic flights are considered to be electrified in these airports. According to the annual air traffic data for UK airports from the UK Civil Aviation Authority (CAA) [20], these airports serve around 37% of the total number of the UK domestic air passengers.

III. ELECTRIC AIRCRAFT CHARGING SYSTEMS

The main energy resources to provide EA charging consist of grid electricity, micro gas turbines, and solar energy (PV), as shown in Fig. 1. There are two technical approaches to recharge the EA batteries. The first approach is to implement fast chargers, which aims to recharge EA batteries during the ground handling process for the flight similar to the fuel refilling. By observing the flight schedule data from London Heathrow Airport, a domestic flight which arrived at the destination airport will be parked at the gate position for 30 to 50 minutes [21]. During this limited time period, the EA batteries are required to be charged with unrealistic high power super-fast chargers (50 MW level chargers for the proposed EA). There are significant technical barriers to develop the chargers for EA, such as power capacity, overheating, battery degradation, and the network constraints. The alternative way is to implement the battery swap process. All EA batteries can be recharged on the ground for a flexible time period and can be swapped to the arrival aircraft in the ground handling process [22]. Due to the technical barriers to develop MW level chargers with long battery charging time which will sequentially delay the flight journey, battery swap is chosen as a suitable technology to integrate into the existing airport operation management in our case studies. Aviation is a highly scheduled transportation, which allows the airport operators to manage the arrival and departure time of aircraft and fit the battery swap process in between. The battery swap process is conducted together with the ordinary cargo loading process, taking around 30 minutes after the EA starting to park at the apron with all the passengers de-boarded [22]. Therefore, the charging schedule is required to be analysed for the economic dispatch of the airport charging system for battery swap process.

Our findings show that 8.7 GWh daily energy consumption is required for electric aircraft charging in the 8 UK airports. Such additional energy consumption is not feasible to be solely provided by grid-level energy supply. Therefore, we have designed the airport gas turbines and microgrid to cover 50% off-grid charging in order to relieve the grid-level energy requirements. In addition, 15% of charging energy is supplied by renewable energy sources. The airport microgrid with combined gas turbine, PV as well as grid-level power supply can be coordinated to provide super-fast charging to meet busy flight schedules.

A. Flight schedule driven charging requirement

Over the past decade, more than 50 all-electric conceptual, experimental, and commercial aircraft have been designed. Although the current battery specific energy level of 250 Wh/kg is not enough for powering a middle size all-electric aircraft, the battery specific energy is potentially to reach 800 Wh/kg in the mid of the century [2]. Based on the research [23], the battery with specific energy of 800 Wh/kg will enable all-electric version A320 to carry 28 MWh battery and transport 180 passengers for a range of 500 nm, which could cover the regional and domestic flight missions in the UK. This is the reason why the year 2050 is envisioned for the commercial all-electric aircraft entering into service for the domestic air transport [2]. In this paper, we use an all-electric aircraft with a battery specific energy of 800Wh/kg, with a 500 nautical-mile design range and 180 passenger capacity, which was designed in [23], to investigate electrified air transport – power grid nexus through the novel concept of Aviation-to-Grid. The technical assumptions of all-electric A320 including the aircraft battery and charging are listed in TABLE I.

TABLE I
THE PARAMETERS OF THE ALL-ELECTRIC AIRCRAFT A320 [23]

Design property	All-electric aircraft
Passenger	180
Distance Range (km/nm)	926/500
Battery Energy (MWh)	28
Nominal charging and discharging power (MW)	5
Charging/discharging efficiency (%)	97

The flight schedules will be analysed to meet the peak EA charging demand. The peak charging hours are determined by the number of chargers available at airport. Based on the flight schedules, there are nearly zero flight during 00:00 to 07:00. In order to guarantee the fully charged batteries for the entire day flights, the 30% of daily energy requirement of all EA batteries is scheduled to be recharged during these 7 hours. The initial number of swappable batteries are set equal to the number of arrival flight at the peak of flight schedule in each airport. The number of chargers could be calculated as follow:

$$N_c = \frac{\beta_e \times E_{batt,tot}}{P_{charger} \cdot T_{night}} \quad (1)$$

where N_c is the number of battery chargers at each airport, β_e is the coefficient of the required energy for charging EA batteries during the 7 hours night period, $P_{charger}$ is the rated power of each battery charger, $E_{batt,tot}$ is the total energy required by the EA batteries of daily scheduled flights, T_{night} is the night charging period defined from 00:00 to 07:00.

The transformer capacity is sized to the peak charging power of the EA on the busiest day of flight schedules. For resilient energy operation, the installed capacity of airport gas turbine is assumed to be equivalent to the grid transformer capacity, to cover the 'N-1' criteria that either the gird transformer or gas turbine outage would still meet the peak EA charging demand.

B. PV capacity and output profile

The estimation for the maximum PV installation capacity is based on the land availability of individual airports. In this paper, car park canopy and building rooftop are considered as ideal locations for PV installation. The PV installation capacity varies with the PV module technologies and type of mounting systems. This work has its main focus on the EA charging system, therefore the PV capacity calculation will only be based on the area of canopy and building rooftop for an initial and high-level estimation. The worldwide standard of PV land size over installed capacity is 1 MW per 2ha (5 acres) which will be used for PV capacity estimation in airport areas [24]. The 2019 PV generation profiles of relevant cities where the

airports are located are calculated based on this model. The PV panels are installed horizontally, which means the installation tilt is 0°. The results for PV installation capacity of 8 UK airports are summarised in TABLE II.

The power output profile of airport PV generation is calculated based on the Global Solar Energy Estimator (GSEE) model [25] with estimated maximum PV installation capacity. The model is developed based on the irradiance data of the PV panels. The PV power output can be calculated by (2).

$$P_{PV,t} = P_{PV}^{max} \frac{r_t}{r^{STC}} [1 + k_T(T_t - T_r)] \quad (2)$$

where $P_{PV,t}$ is the power output of the PV cell at time t. P_{PV}^{max} is the maximum installation capacity of the PV cell under the standard test condition (1,000 W/m², 25℃). r_t is the light intensity of the PV cell at time t. r^{STC} is the standard test light intensity of the PV cell, equals 1,000 W/m². k_T is the power temperature coefficient. T_t is the temperature of the PV cell. T_r is the reference temperature.

C. Gas turbine operation parameters

The power output of the gas turbine can be calculated as (3).

$$P_{GT,t} = \eta_{GT} \cdot G_{GT,t} \quad (3)$$

where $P_{GT,t}$ is the power output of the gas turbine at time t. η_{GT} is the efficiency of the gas turbine. $G_{GT,t}$ is the gas input at time t.

In order to achieve the switch-on and switch-off control for gas turbine scheduling, the gas turbine sate flow model [26] is adopted. The operation status of gas turbine including the switch control is modelled in equation (4-8), where the following state binary variables are introduced: operation state variable v_t, starting up integer variable y_t, and shutting down integer variable z_t. The transition between the variables are formulated:

$$y_t - z_t = v_t - v_{t-1} \quad (4)$$
$$y_t + z_t \leq 1 \quad (5)$$
$$\lambda_{GT,min} \cdot P_{GT}^{max} \cdot v_t \leq P_{GT,t} \leq \lambda_{GT,max} \cdot P_{GT}^{max} \cdot v_t \quad (6)$$
$$RD \cdot v_{t-1} \leq P_{GT,t} - P_{GT,t-1} \leq RU \cdot v_t \quad (7)$$
$$UT \cdot y_t \leq \sum_{l=k}^{k+UT} v_l \leq DT \cdot (1 - z_t) \quad (8)$$

Constraints (6) and (7) formulates the operation boundaries of the gas turbine. The necessary start-up time of gas turbine is also taken into consideration by the equation (8). The parameters of the gas turbines can be found in [15].

D. Battery swap state flow model

The Mathematical formulation of battery swap process is a typical job-shop problem that can be described by the state flow

TABLE II
SIZING OF EA CHARGING EQUIPMENT AND AIRPORT ENERGY RESOURCES

Airport	IATA Code	Total Area (acres)	Available Area (acres)	Grid (MVA)	PV (MW)	GT (MW)	Num. of Batteries	Num. of Chargers
London Heathrow	LHR	3,032	250	180	50	180	260	36
Edinburgh	EDI	1,300	85	170	17	170	240	34
Glasgow	GLA	1,028	37	120	7	120	170	24
Manchester	MAN	1,384	88	85	17	85	120	17
Birmingham International	BHX	820	108	60	21	60	80	12
Belfast International	BFS	1,198	58	60	11	60	80	12
London Gatwick	LGW	1,665	217	45	43	45	60	9
London Stansted	STN	1,796	95	35	19	35	50	7

model [13]. In this work, the battery swap state flow model developed in the literature is utilised to model the EA battery swap process, which is formulated as follow:

$$\sum_{i}^{T_c}\left(n_{c,t}^i + n_{w,t}^i\right) + n_{f,t} = N_b \tag{9}$$

$$n_{dc,t}^i + n_{dw,t}^i = n_{d,t-T_{bs}}^i \tag{10}$$

$$n_{c,t}^i = n_{c,t-1}^{i-1} + n_{dc,t-1}^{i-1} + n_{wc,t}^i \tag{11}$$

$$n_{w,t}^i = n_{w,t-1}^{i-1} + n_{dw,t-1}^{i-1} - n_{wc,t}^i \tag{12}$$

$$n_{f,t} = n_{f,t-1} + n_{c,t}^{T_c} - \sum_{i}^{T_c}\left(n_{d,t}^i\right) \tag{13}$$

$$\sum_{i}^{T_c}\left(n_{c,t}^i\right) \le N_c \tag{14}$$

$$n_{c,1}^i = n_{c,T}^i, n_{w,1}^i = n_{w,T}^i, n_{f,1} = n_{f,T} \tag{15}$$

Eq. (9) represents the balance of total number of batteries. The total number of batteries N_b is constant in three charging states including charging $n_{c,t}^i$, fully charged $n_{f,t}$ and empty batteries $n_{w,t}^i$ in an airport. The constraint (10) defines the battery swapping process. After the time T_{bs} spent on battery swapping, the depleted batteries entering the airport are divided into two groups: direct charge group $n_{dc,t}^i$, and waiting for charge group $n_{dw,t}^i$. The charging and waiting batteries could be calculated as constraints (11) and (12), $n_{wc,t}^i$ is the number of batteries transferring from waiting to charging state at time t. The number of fully charged batteries is calculated by sum up the number of fully charged batteries and minus the depleted (swapped) batteries $\sum_{i}^{T_c}\left(n_{d,t}^i\right)$. Due to the repetitive operation pattern of daily airport battery swapping process, the number of batteries with SoC in each state are equal between the beginning and end of the day, formulated as (13-15). All of the variables in Eq. (9)-(15) to represent the number of batteries are integer.

E. Electrical power balance

The total charging demand of EA battery can be calculated from the number of charging batteries and the rated power of battery chargers.

$$P_{c,t} = \sum_{i}^{T_c}\left(n_{c,t}^i\right) \cdot P_{charger} \cdot \eta_c \tag{16}$$

where $P_{c,t}$ is the power output of battery chargers. η_c is the charging efficiency of EA batteries.

The power generated from the grid, gas turbines and the PV panels are balanced with the EA charging demand.

$$P_{grid,t} + P_{PV,t} + P_{GT,t} = P_{c,t} \tag{17}$$

where $P_{grid,t}$ is the power import from the grid, $P_{PV,t}$ is the power generated by PV, $P_{GT,t}$ is the power generated by the gas turbine.

The power output of each airport energy source should be within their capacity:

$$0 \le P_{unit,t} \le P_{unit}^{max}, \ unit = PV, grid, GT \tag{18}$$

IV. AVIATION-TO-GRID FREQUENCY RESPONSE

EA charging system is innovatively utilised to provide primary and secondary frequency response through the EA batteries and airport gas turbine. As shown in Fig. 1, an energy control strategy is developed to dispatch EA batteries and gas turbines by monitoring the real-time system frequency, and a

frequency response control is set up to mitigate frequency deviation. The EA charging scheme will be scheduled on an hourly basis by the flight schedule with battery swap process.

A. Objective function of EA charging system operation with A2G frequency response

The electric aircraft charging scheduling problem is formulated as a mixed-integer linear programming (MILP) optimisation problem. The objective function is to minimize the total energy operation costs of the airport EA charging system. The costs include the electricity purchase cost from the grid, the gas supply cost and the frequency response revenue. The calculation method for the frequency response revenue is shown in Eq. (19-20).

$$Obj = min\left(\sum_{s=1}^{2} d_s(OC_s - R_{A2G,s})\right) \tag{19}$$

$$OC_s = \sum_{t=1}^{T}\left(P_{grid,s,t} \cdot p_e + G_{GT,s,t} \cdot p_g\right) \cdot \Delta t \tag{20}$$

where OC_s is the operation costs of EA charging system. p_e is the time-of-use electricity price. p_g is the gas price. d_s is the number of days in one season (230 days for summer, 135 days for winter).

Firm Frequency Response (FFR) is triggered when grid frequency drops below a specific threshold of 49.7Hz [27]. The charging batteries will reverse the charging state to discharging and consequently to provide double volume of frequency response to its rated power. All batteries are required to sustain their output for 30s as required by primary response, then the batteries are linearly reduced their output at the rate of 0.5 MW/s in order to prevent instantaneous power imbalance [31][32]. The primary response will require the batteries to discharge for only 30 seconds, hence the batteries state of charge (SoC) will be estimated to reduce by less than 5%, which will not affect the scheduled flight operation.

The gas turbine can participate in both primary and secondary frequency control as long as the operation reserve of gas turbine is available [30]. The primary frequency control requires the gas turbine to automatically increase (or decrease) power output within a certain timescale when a grid frequency event occurs. A commonly used frequency response requirement is used to achieve 50% power output within 15 seconds and 100% within 30 seconds proposed by European Grid Authorities [31]. The secondary response is then provided by the gas turbine to sustain the system frequency for 30 minutes. The total primary response power and secondary reserve energy can be calculated by (21-24).

$$\Delta P_{B,t}^{res} = 2 \cdot P_{c,t} \tag{21}$$

$$0 \le \Delta P_{GT,t}^{res} \le \varphi \cdot P_{GT}^{max} \cdot v_t \tag{22}$$

$$\Delta P_{A2G,t} = \Delta P_{B,t}^{res} + \Delta P_{GT,t}^{res} \tag{23}$$

$$E_{A2G,t} = \Delta P_{GT,t}^{res} \cdot T_s \tag{24}$$

where φ denotes maximum reserve power proportion of gas turbines, $\Delta P_{B,t}^{res}$ is the response power from the EA batteries. $\Delta P_{A2G,t}$ is the A2G primary response power. $E_{A2G,t}$ is the A2G secondary reserve energy, $\Delta P_{GT,t}^{res}$ is the response power from gas turbines. T_s is the response time of gas turbine, which is 30 minutes.
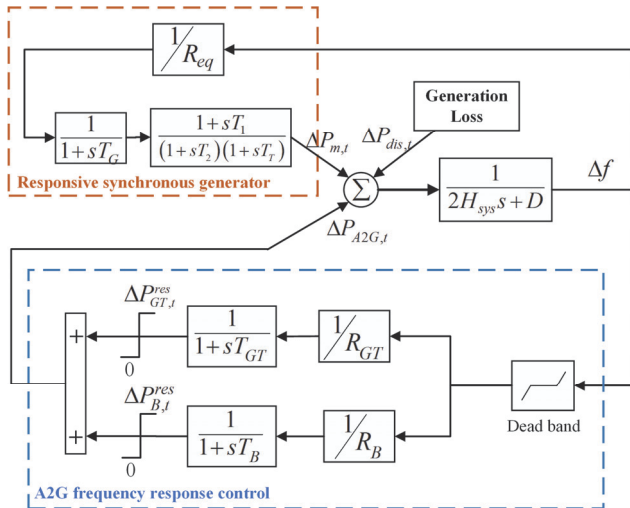
Fig. 2. Simplified GB power system model with the A2G frequency response control

The FFR contract with GB National Grid will stipulate a revenue settled in every half an hour. The primary and secondary response reserve revenue will be paid by a fixed tariff. The price will be paid like an insurance even in a normal operation with no frequency events [32]. The frequency response revenue is calculated in Eq. (25).

$$R_{A2G,s} = \sum_{t=1}^{T} \left(\Delta P_{A2G,t} \cdot p_{pri} + E_{sec,s,t} \cdot p_{sec} \right) \cdot \Delta t \quad (25)$$

where $R_{A2G,s}$ is the daily A2G frequency response revenue in summer or winter season. p_{pri} and p_{sec} are the primary and secondary frequency response revenue respectively.

B. A2G frequency response integration to power system

After solving the MILP optimisation problem, the results of A2G frequency response powers ($\Delta P_{B,t}^{res}$ and $\Delta P_{GT,t}^{res}$) are put into the frequency response simulation model to derive the frequency response results. As shown in Fig. 2, the simplified Great Britain (GB) power system with inertia estimation [5] was used to analyse the frequency response from the EA charging system. The parameters of the simplified GB power system can be found in [16]. The time evolution of system frequency deviation can be described by a first-order ordinary differential equation in Eq. (26) [5].

$$2H_{sys} \frac{\partial \Delta f_t}{\partial t} + D * P_t^D * \Delta f_t = \Delta P_{m,t} - \Delta P_{dis,t} + \Delta P_{A2G,t} \quad (26)$$

where Δf_t is the frequency deviation at time t, P_t^D (MW) is the power system demand level, and $\Delta P_{dis,t}$ is the generation power loss, $\Delta P_{m,t}$ is the response power from synchronous generators. The H_{sys} (MW/Hz) is the power system inertia constant, which represents the total stored kinetic energy in the synchronous generators of the power system.

The synchronous generators are modelled by a governor droop block, a governor actuator block, and a turbine block. T_G is the typical governor actuator time constant of 0.2s. A transient droop compensation is introduced between the governor and the turbine which is a lead-lag transfer function with time constants T_1 and T_2 at 2s and 12s respectively. The turbine model is characterized by a time constant T_T of 0.3s, which represents the mechanical power output following the

governor action. D (%/Hz) is a single damping constant which represents the damping provided by the frequency-dependent loads. These parameters capture the characteristics of different governors and turbines in response to a frequency change, which can be derived from a frequency deviation event caused by power imbalance [16]. The responsive synchronous generators are represented by the closed-loop transfer functions (27-28).

$$G_g(s) = \frac{1}{1 + s \cdot T_G} \quad (27)$$

$$G_T(s) = \frac{1 + s \cdot T_1}{1 + s \cdot T_2 T_T + s^2 \cdot (T_2 + T_T)} \quad (28)$$

The A2G frequency response system includes gas turbines and EA batteries. Both the gas turbines and EA batteries will provide a primary response by adopting droop control, then the gas turbines will keep at a constant power to provide a secondary response. When the meters sense the system frequency falls below 49.7 Hz, the reserve power will be discharged to the power system. The dynamic model can be formulated by the following first-order equations:

$$\frac{\partial \Delta P_{u,t}}{\partial t} = \frac{1}{T_u} \left(-\frac{\Delta f_t}{R_u} - \Delta P_{u,t} \right) , (u = B, GT) \quad (29)$$

$$\Delta P_{A2G,t} = \sum_u \Delta P_{u,t} , (u = B, GT) \quad (30)$$

where $\Delta P_{u,t}$ is the response power output from the units (EA batteries and gas turbines). T_u and R_u are the time delay constant and the droop constant for the EA batteries and gas turbines to inject response power to grid.

V. RESULTS AND DISCUSSION

A. Case studies with input data and assumptions

The sizing of EA charging system is shown in TABLE II. The A2G frequency response control system and the simplified GB power system are modelled on the Simulink platform of MATLAB 2019b. The electric aircraft charging scheduling problem is solved by the MILP algorithm in CPLEX solver. The modelling process is conducted on a PC with Intel Core i5-8500 CPU @ 3.00 GHz and 8 GB RAM. As discussed in the previous section, the flight schedules vary with seasonal effect. In the case studies, two weeks' flight schedules in summer peak month (May) and winter peak month (November) are investigated. In this paper, the inertia of the GB power system is based on the long-term inertia forecast of a typical value 100 GVA·s in 2050 across both summer and winter for the simplification purpose [33]. T_B is assumed to be 35 ms that is similar to the normal EV charging case [17]. T_{GT} is set at 10s according to reference [34]. The maximum reserve power proportion of gas turbines is assumed to be 15%. The droop constants of the EA batteries and gas turbines are assumed to be 2.5% and 5% respectively. The national demand profiles on a typical summer and winter day are utilised in the case studies. The total power system demands are 41.6 GW as the winter maximum demand and 21.2 GW as the summer minimum demand. The simulated generator loss is assumed at 1,800 MW, which is equivalent to the largest generators loss at Sizewell nuclear power station in the UK. The power loss is assumed to happen repeatedly in every 30 minutes interval. For airport

energy purchase from grid, the gas price is stable at 0.038 £/kWh, while the time of use (TOU) pricing mechanism of electricity price is introduced as £0.07 (00:00-07:00), £0.15 (10:30-16:00 and 21:00-24:00), and £0.2 (07:00-10:30 and 16:00-21:00) per kWh. The primary A2G frequency will receive a stable capacity revenue which is assumed to be 8 £/MW per 30 min. The secondary response power will receive a payment for reserved energy (10 £/MWh per 30 min).

B. Energy dispatch results of EA charging system

Fig. 3 shows the hourly EA charging supply and demand driven by the power generation dispatch with defined flight schedules. The results indicate that the EA charging demand patterns are different to the flight schedules due to the battery swap with optimal energy dispatch that enables the charging demand flexibility in the airport operation. In terms of power generation, the power drawn from the grid is significantly high during the night from 00:00 to 07:00, while gas turbines supply the most EA charging demand during the daytime and in the evening. This is because the electricity price is cheaper during the night which incentivises the EA charging system to purchase electricity from grid to fully change batteries for the oncoming flight missions. The advantage of this EA charging arrangement is to compensate the national power system demand profiles across the 8 UK airports, where the overnight national demand valley can be filled by EA charging, while the day and evening demand peak can be self-dispatched by airport gas turbines. To maximise the PV generation, the EA charging system dispatches the maximum available PV generation during the daytime, which ensures the 100% utilisation of renewable PV generation. Due to the seasonal effect of solar energy source in particular the output reduction over winter period, gas turbines are operating at a higher level in the winter daytime.
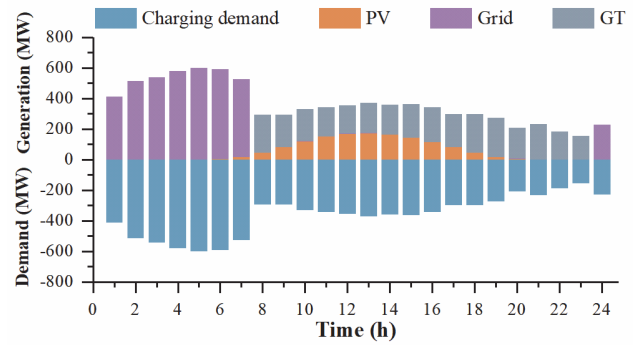
C. A2G frequency response results

Fig. 3. Energy dispatch results of the 8 UK airports

The A2G frequency control mechanism is triggered when a frequency deviation such as power generation loss occurs. Fig. 4 (e) and (f) show a series of frequency nadirs – the minimum post-contingency frequency after the system suffers a loss of 1,800 MW generation in every 30 minutes interval with and without A2G frequency response. Comparing with the without A2G scenario, the half-hourly frequency nadir improved significantly by approximately 0.4 Hz during the night and 0.2 Hz in the day. The effectiveness of A2G frequency response in improving frequency nadir is dependent on the power system inertia, and A2G becomes more effective in the summer and 00:00-07:00 period due to the weak system inertia. When the frequency event occurs, the charging batteries not only stop charging but also being able to fully discharge the power back to the grid. This makes the "double effect" of frequency response capacity. Therefore the night frequency nadir improved twice as much as daytime due to the EA batteries which are fully available to provide frequency response 00:00-07:00 when no flights are scheduled. During the daytime the frequency response is mainly provided by gas turbines. In a realistic power system operation scenario, the frequency contingency events will not happen repeatedly at such a short interval. As a result, this study
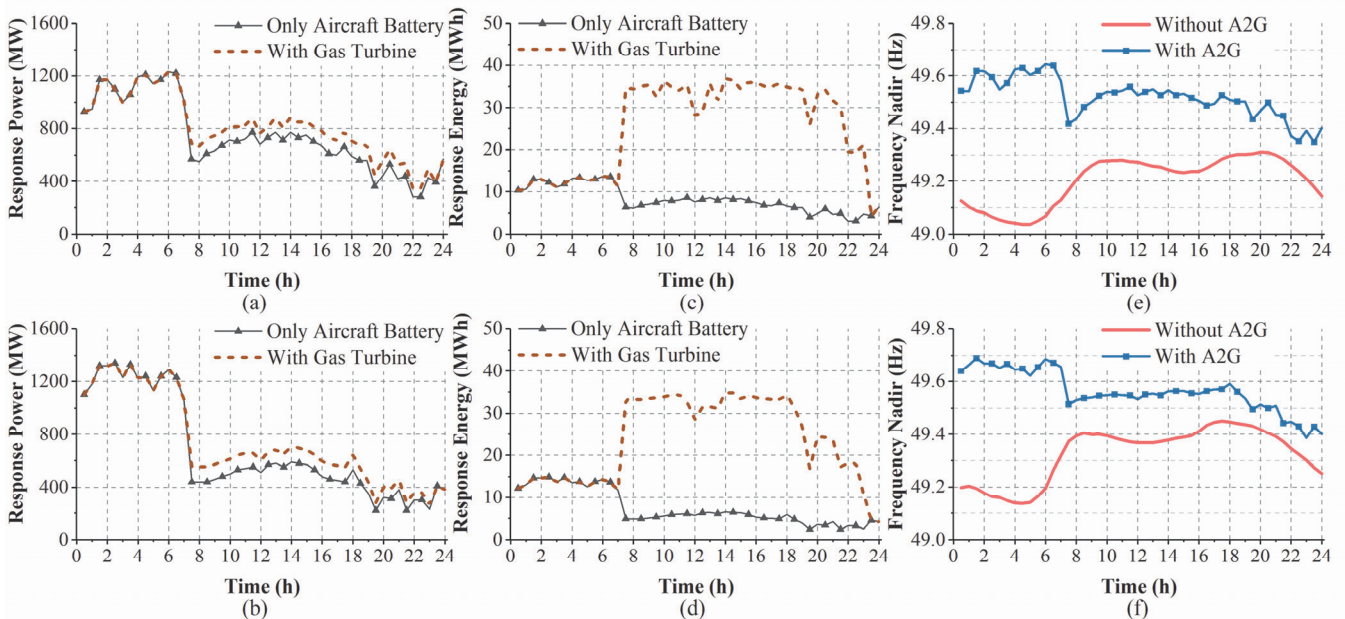

Fig. 4. Frequency response power and energy from the EA batteries and gas turbine. (a) response power (summer), (b) response power (winter), (c) response energy (summer), (d) response energy (winter), (e) Frequency nadir (summer), (f) Frequency nadir (winter)

always assumes that each frequency events in a half-hourly interval are independent and there is sufficient power reserve capacity to restore the frequency before the next contingency event. Overall, the average frequency nadir can be improved by 0.31 Hz in summer, and 0.23 Hz in winter due to the A2G frequency response services. Most importantly, the number of Infrequent Infeed Loss Risk (defined as below 49.5 Hz [28]) can be reduced by 83.33% in summer and 68.75% in winter, which significantly reduce the likelihood of significant frequency deviations with A2G frequency response services.

D. Response power and energy from A2G system

The amount of response power available from A2G frequency response through EA batteries and airport gas turbines is calculated, and the results are shown at every half an hour for a summer and winter day in Fig. 4 (a-b). There are 900 to 1,200 MW response power capacity from 00:00 to 06:30 when there is no flight, and 300 to 900 MW capacity when the EA requires charging power. The higher power response capacity during night is caused by the full amount of EA batteries that are available at airports overnight. In the peak flight scheduling periods of 20:00 - 22:00 in summer and 19:00 - 21:00 in winter, the majority of EA batteries are used to meet aviation requirements, therefore less power response capacity is observed. Such response power capacity has a strong impact by the EA charging schedules. To discuss the response power capacity from different sources, the EA batteries provide 100% of response power capacity overnight and around 80% - 90% capacity during the day, gas turbines can only provide around 10% to 20% response power capacity from 07:00 to 23:00. This is because the response power of gas turbines for frequency control can only provide response power when the turbines are dispatched. Overnight due to the low electricity price, the charging power is mainly from the external power grid with no gas turbines dispatchable overnight to provide response power capacity. For the rest of time, the A2G system provides a combined response power from EA batteries and gas turbines.

The response energy provided by EA batteries and gas turbines is calculated in Fig. 4 (c) and (d). Gas turbines can provide more than 30 MWh response energy on most occasions, with peak response energy of 35 MWh in both summer and winter. However, the EA batteries can only provide response energy around 10 to 15 MWh (overnight) and 5 to 10 MWh (daytime). The reason for gas turbine to provide much higher response energy is due to the sustained power output of gas turbine over a longer period of 30 minutes comparing with the constrained response time of only 30 seconds for EA batteries. The response energy provided by gas turbines is up to four times higher than EA batteries.

E. Response revenue and charging costs

The annual EA charging costs with A2G frequency response revenue are shown in Fig. 5. The EA charging costs consist of

two main parts: the grid electricity purchase and the gas turbine energy consumption, which are based on the electricity and gas prices provided. The calculated EA charging costs across 8 UK airports demonstrate a balanced expenditure on electricity and gas usage for all airport size with flight schedule variation. The annual frequency response revenue is calculated in equations (27). In average, the frequency response revenue can off-set 19.8% to 30% of charging costs across 8 UK airports. The total revenue generated from A2G frequency response services is estimated at £46.58 million.
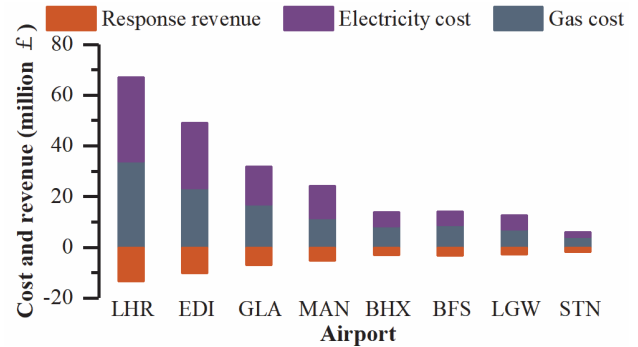

Fig. 5. Annual EA charging costs and A2G frequency response revenue for 8 UK airports

F. Sensitivity analysis of A2G generation capacity

Sensitivity analysis has been conducted to investigate the impacts of generation capacity on the energy dispatch of EA charging system, associated with A2G frequency response power and energy. Additional two scenarios are considered as scenario 2 - half gas turbine capacity, and scenario 3 - half grid transformer capacity.

Fig. 6 shows the response power and energy that are provided by the 50% reduced capacity of gas turbine or grid transformer, together with the frequency nadir simulation results subject to half-hourly power loss events. Scenario 2 (half gas turbine) demonstrates uneven distribution of response power across day and night, and less response energy due to the 50% reduced participation of gas turbine in providing sustained response energy to the secondary response timescales. Scenario 3 shows 0-180 MW lower response power during the night and 0-160MW higher response power during the day. This is due to the increased gas turbine participation in energy dispatch when the grid supply capacity drops to half, which will smooth out the response power and energy between day and night. However, base case scenario with balanced grid and gas turbine capacity is still considered as an optimal option due to the higher response power provided for low system inertia period. Such frequency phenomenon can be observed in 24 hours' frequency nadir results that base case with balanced generation capacity will effectively manage frequency nadirs for both day and night (Fig. 6 c).
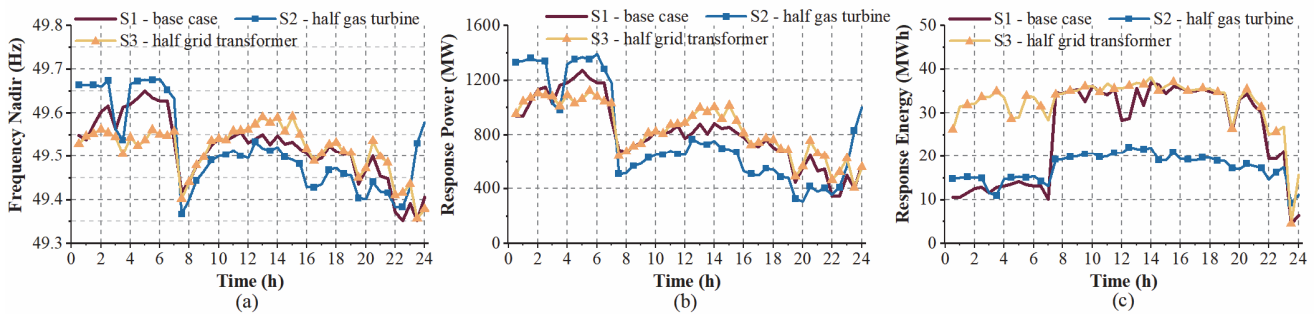
G. Grid service value

Fig. 6. Frequency nadir (a), response power (b), and response energy (c) by reduced generation capacity of grid electricity and gas turbine
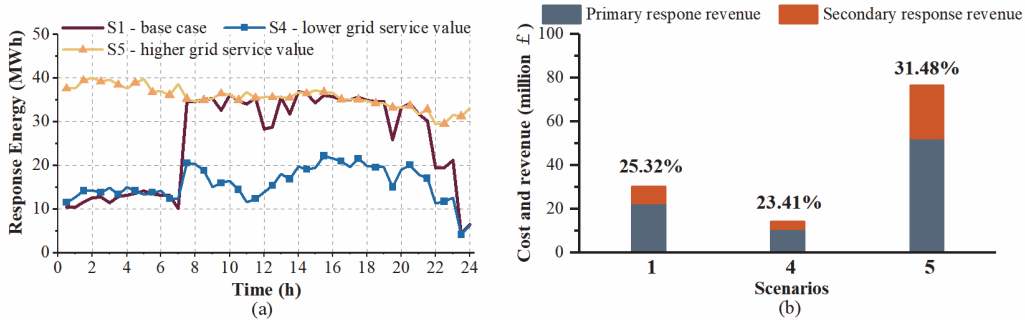

Fig. 7. Response energy (a) and response revenue (b) of case studies with lower and higher grid service values

Sensitivity analysis of grid service value on energy dispatch strategy and frequency response revenue is conducted. Scenario 1 as a base case with primary response payment of 8 £/MW and secondary response payment of 10 £/MWh. Scenario 4 and scenario 5 are new case studies to represent lower and higher grid service values. In lower grid service value, the response payments is assumed to become half: 4 £/MW for primary response and 5 £/MWh for secondary response. In higher grid service value, the response payments are doubled: 16 £/MW for primary response and 20 £/MWh for secondary response.

In Fig. 7 (a), higher grid service value leads to more response energy to be dispatched from A2G system, in particular overnight when the gas turbine is on secondary response. Lower grid service value discourages response energy by half comparing with base case scenario. In Fig. 7 (b), frequency response revenues are compared across three scenarios with different shares between primary and secondary response. Higher grid service value will attract higher frequency response revenue, because both value and capacity of frequency response are increased. Furthermore, secondary response revenue which is primarily provided by gas turbine is more sensitive to the variation of grid service value.

VI. CONCLUSION

The electrification of aviation enables the electric aircraft (EA) charging to provide valuable flexibility services to the power grid. This paper proposes a new concept of Aviation-to-Grid (A2G) flexibility that utilises EA charging system with battery swap method to provide grid frequency response services. Smart EA charging system is developed to dispatch PV, gas turbine and grid electricity in order to meet EA charging demand associated with the seasonal flight schedules. The A2G frequency response system is developed to coordinate

primary and secondary frequency response control with the grid inertia estimation. The hourly energy dispatch strategy is optimised to achieve the minimum operation costs by considering the EA charging demand, energy prices and A2G frequency response revenue. Case studies are conducted in 8 UK airports which serve around 37% of the total UK domestic air passengers. The results show that the typical A2G frequency response services capacity across the 8 UK airports can reach between 900 - 1,300 MW overnight and 200 - 900 MW daytime with seasonal variation. EA batteries can provide frequency response power up to six times higher than gas turbine during the day, while 100% of frequency response power is provide by EA batteries overnight. However, gas turbine can provide approximately four times higher frequency response energy than EA batteries due to the sustained gas turbine output. The installed generation capacity has a significant impact on the energy dispatch strategy, and response power and energy of A2G frequency response system. The annual revenue that is generated from A2G frequency response is estimated to be £46.58 million, which can cover 19.8% to 30% of energy consumption costs of EA charging in future airports. The average frequency nadir can be improved by 0.31 Hz in summer and 0.23 Hz in winter due to the A2G frequency response services, and the likelihood of Infrequent Infeed Loss Risk (defined as power system frequency below 49.5 Hz) can be reduced by 83.33% in summer and 68.75% in winter. The sensitivity analysis of grid service value reveals that the higher grid service value will attract higher frequency response revenue. Specifically, the secondary response revenue which is provided by gas turbine is more sensitive to the variation of grid service value.

For future work, the airport charging infrastructure will be designed, and cost-benefit analysis will be conducted for the full EA charging system project cycle from design to operation.

Uncertainties will be introduced in flight schedules, energy dispatch and daily airport operation.

REFERENCES

[1] G. Buticchi, M. Liserre, and K. Al-Haddad, 'On-Board Microgrids for the More Electric Aircraft', *IEEE Trans. Ind. Electron.*, vol. 66, no. 7, pp. 5585–5587, 2019, doi: 10.1109/TIE.2019.2897470.

[2] A. W. Schäfer *et al.*, 'Technological, economic and environmental prospects of all-electric aircraft', *Nat. Energy*, vol. 4, no. 2, pp. 160–166, 2019, doi: 10.1038/s41560-018-0294-x.

[3] National Grid ESO, 'Technical Report on the events of 9 August 2019', 2019. [Online]. Available: https://www.nationalgrideso.com/document/152346/download. [Accessed: 08-Oct-2021].

[4] National Grid, 'Future Energy Scenarios Navigation', 2020. [Online]. Available: https://www.nationalgrideso.com/future-energy/future-energy-scenarios/fes-2020-documents. [Accessed: 13-Nov-2020].

[5] P. Kundur, *Power System Stability And Control*, 1st ed. McGraw-Hill Education, 1994.

[6] L. Mehigan, D. Al Kez, S. Collins, A. Foley, B. Ó'Gallachóir, and P. Deane, 'Renewables in the European power system and the impact on system rotational inertia', *Energy*, vol. 203, p. 117776, 2020, doi: 10.1016/j.energy.2020.117776.

[7] F. Teng, Y. Mu, H. Jia, J. Wu, P. Zeng, and G. Strbac, 'Challenges on primary frequency control and potential solution from EVs in the future GB electricity system', *Appl. Energy*, vol. 194, pp. 353–362, 2017, doi: 10.1016/j.apenergy.2016.05.123.

[8] Z. A. Obaid, L. M. Cipcigan, and M. T. Muhssin, 'Fuzzy hierarchal approach-based optimal frequency control in the Great Britain power system', *Electr. Power Syst. Res.*, vol. 141, pp. 529–537, 2016, doi: 10.1016/j.epsr.2016.08.032.

[9] U. Sultana, A. B. Khairuddin, B. Sultana, N. Rasheed, S. H. Qazi, and N. R. Malik, 'Placement and sizing of multiple distributed generation and battery swapping stations using grasshopper optimizer algorithm', *Energy*, 2018, doi: 10.1016/j.energy.2018.09.083.

[10] W. Jie, J. Yang, M. Zhang, and Y. Huang, 'The two-echelon capacitated electric vehicle routing problem with battery swapping stations: Formulation and efficient methodology', *Eur. J. Oper. Res.*, 2019, doi: 10.1016/j.ejor.2018.07.002.

[11] C. Y. Justin, A. P. Payan, S. I. Briceno, B. J. German, and D. N. Mavris, 'Power optimized battery swap and recharge strategies for electric aircraft operations', *Transp. Res. Part C Emerg. Technol.*, vol. 115, no. July 2019, p. 102605, 2020, doi: 10.1016/j.trc.2020.02.027.

[12] Y. Cheng and C. Zhang, 'Configuration and operation combined optimization for EV battery swapping station considering PV consumption bundling', *Prot. Control Mod. Power Syst.*, vol. 2, no. 1, Dec. 2017, doi: 10.1186/s41601-017-0056-y.

[13] N. Liu, Q. Chen, X. Lu, J. Liu, and J. Zhang, 'A Charging Strategy for PV-Based Battery Switch Stations Considering Service Availability and Self-Consumption of PV Energy', *IEEE Trans. Ind. Electron.*, vol. 62, no. 8, pp. 4878–4889, 2015, doi: 10.1109/TIE.2015.2404316.

[14] B. Sun, X. Sun, D. H. K. Tsang, and W. Whitt, 'Optimal battery purchasing and charging strategy at electric vehicle battery swap stations', *Eur. J. Oper. Res.*, vol. 279, no. 2, pp. 524–539, 2019, doi: 10.1016/j.ejor.2019.06.019.

[15] M. A. Gonzalez-salazar, T. Kirsten, and L. Prchlik, 'Review of the operational flexibility and emissions of gas- and coal-fired power plants in a future with growing renewables', *Renew. Sustain. Energy Rev.*, vol. 82, no. July 2017, pp. 1497–1513, 2018, doi: 10.1016/j.rser.2017.05.278.

[16] Y. Mu, J. Wu, J. Ekanayake, N. Jenkins, and H. Jia, 'Primary frequency response from electric vehicles in the Great Britain power system', *IEEE Trans. Smart Grid*, 2013, doi: 10.1109/TSG.2012.2220867.

[17] J. Meng, Y. Mu, H. Jia, J. Wu, X. Yu, and B. Qu, 'Dynamic frequency response from electric vehicles considering travelling behavior in the Great Britain power system', *Appl. Energy*, vol. 162, pp. 966–979, 2016, doi: 10.1016/j.apenergy.2015.10.159.

[18] M. Chaoxu, L. Weiqiang, and X. Wei, 'Hierarchically Adaptive Frequency Control for an EV-Integrated Smart Grid With Renewable Energy', *IEEE Trans. Ind. Informatics*, vol. 14, no. 9, pp. 4254–4263, 2018.

[19] Z. Guo, X. Zhang, N. Balta-Ozkan, and P. Luk, 'Aviation to Grid: Airport Charging Infrastructure for Electric Aircraft', *Proc. 12th Int. Conf. Appl. Energy, Thailand/Virtual, Part 2*, vol. 10, 2021.

[20] 'UK Civil Aviation Authority (CAA)'. [Online]. Available: https://www.caa.co.uk/home/.

[21] 'FlightStats - Global Flight Status & Tracker, Airport Weather and Delays'. [Online]. Available: https://www.flightstats.com/v2/. [Accessed: 27-Jun-2020].

[22] M. Schmidt, A. Paul, M. Cole, and K. O. Ploetner, 'Challenges for ground operations arising from aircraft concepts using alternative energy', *J. Air Transp. Manag.*, 2016, doi: 10.1016/j.jairtraman.2016.04.023.

[23] A. R. Gnadt, R. L. Speth, J. S. Sabnis, and S. R. H. Barrett, 'Technical and environmental assessment of all-electric 180-passenger commercial aircraft', *Prog. Aerosp. Sci.*, vol. 105, no. November 2018, pp. 1–30, 2019, doi: 10.1016/j.paerosci.2018.11.002.

[24] 'Topic 13 – Solar Power Plant Installations In Malaysia | AER'. [Online]. Available: http://aer.global/topic-13-solar-power-plant-installations-in-malaysia/. [Accessed: 13-Sep-2020].

[25] S. Pfenninger and I. Staffell, 'Long-term patterns of European PV output using 30 years of validated hourly reanalysis and satellite data', *Energy*, 2016, doi: 10.1016/j.energy.2016.08.060.

[26] B. I. Ayuyev, P. M. Yerokhin, N. G. Shubin, V. G. Neujmin, and A. A. Alexandrov, 'Unit commitment with network constraints', *2005 IEEE Russ. Power Tech, PowerTech*, 2005, doi: 10.1109/PTC.2005.4524780.

[27] Z. Liu, Q. Wu, M. Shahidehpour, C. Li, S. Huang, and W. Wei, 'Transactive real-time electric vehicle charging management for commercial buildings with PV on-site generation', *IEEE Trans. Smart Grid*, vol. 10, no. 5, pp. 4939–4950, 2019, doi: 10.1109/TSG.2018.2871171.

[28] 'THE GRID CODE ISSUE 6 REVISION 6', *National Grid*, 2021. [Online]. Available: https://www.nationalgrideso.com/document/162271/download. [Accessed: 12-Sep-2021].

[29] 'Appendices to the Technical Report on the events of 9 August 2019', 2019. [Online]. Available: https://www.nationalgrideso.com/document/152351/download. [Accessed: 08-Oct-2021].

[30] J. Morren, S. W. H. De Haan, and J. A. Ferreira, 'Contribution of DG units to primary frequency control', *Eur. Trans. Electr. Power*, vol. 16, no. 5, pp. 507–521, 2006, doi: 10.1002/etep.113.

[31] J. DiCampli and W. Schulke, 'Grid stability - Gas turbines for primary reserve', *Proc. ASME Turbo Expo*, vol. 4, pp. 1–9, 2013, doi: 10.1115/GT2013-94466.

[32] 'Firm frequency response (FFR) | National Grid ESO'. [Online]. Available: https://www.nationalgrideso.com/industry-information/balancing-services/frequency-response-services/firm-frequency-response-ffr?overview. [Accessed: 19-Sep-2021].

[33] National Grid ESO, 'Operating a Low Inertia System', 2020. [Online]. Available: https://www.nationalgrideso.com/research-publications/system-operability-framework-sof. [Accessed: 10-Oct-2021].

[34] Y. Zhu and K. Tomsovic, 'Development of models for analyzing the load-following performance of microturbines and fuel cells', *Electr. Power Syst. Res.*, vol. 62, no. 1, pp. 1–11, 2002, doi: 10.1016/S0378-7796(02)00033-0.

2021-10-16

Aviation-to-grid flexibility through electric aircraft charging

Guo, Zekun

IEEE